Gamma radiation: a probe for exploring terrestrial environment

Matteo Albéri

Supervisor: Prof. Fabio Mantovani

Ph.D. in Physics – Cycle XXX Ferrara 28 February 2018

Summary

- **Challenges in outdoor gamma ray spectroscopy**
- **Sources of uncertainties in Airborne Gamma Ray Spectroscopy (AGRS): flight altitude, cosmic radiation, aircraft radioactivity and atmospheric radon**
- **Proximal gamma ray spectroscopy applied to precision agriculture**
- **Conclusions and perspectives**

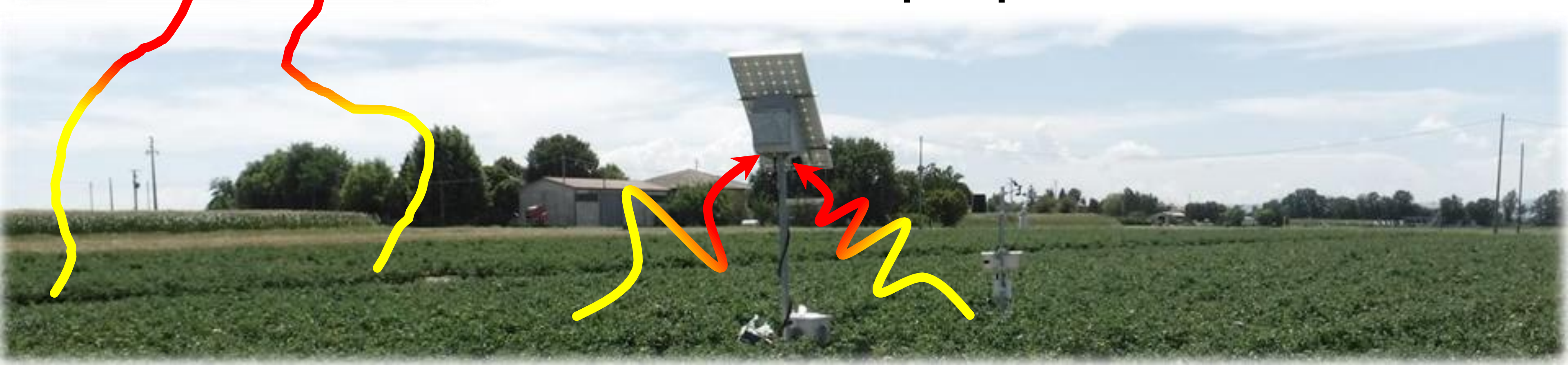

Radionuclides of terrestrial origin investigated with gamma-ray spectroscopy

Isotope	Daughter	Energy (keV)	Half life	Typical abund.
^{40}K	/	1460	1.3 Gy	0.02 g/g
^{238}U	^{214}Bi	1765	4.5 Gy	3 µg/g
^{232}Th	^{208}Tl	2614	14.1 Gy	10 µg/g

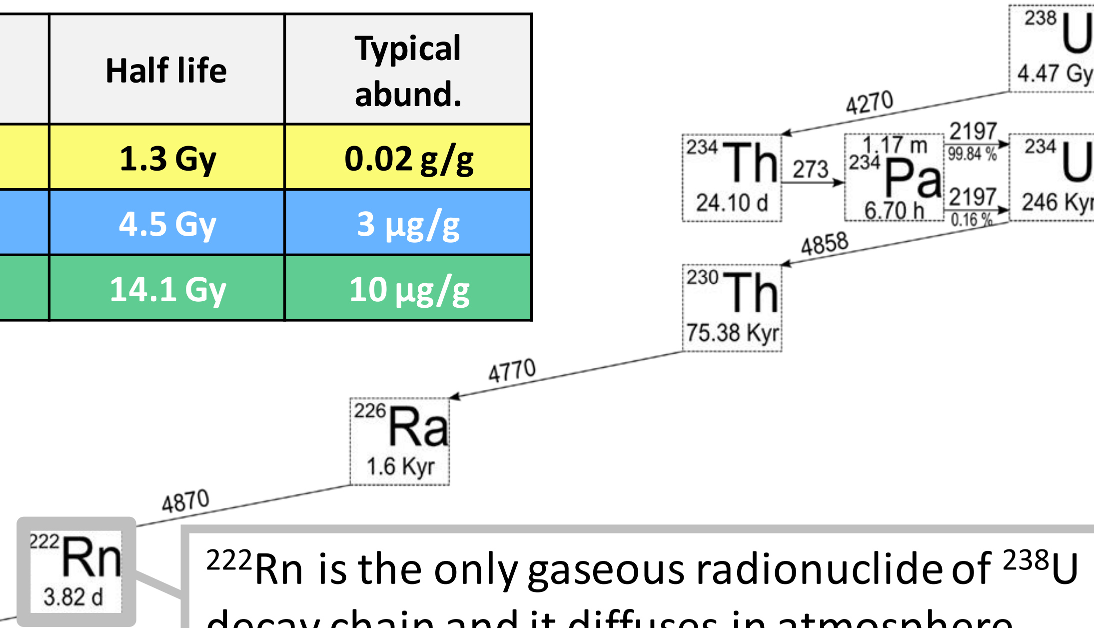

^{222}Rn is the only gaseous radionuclide of ^{238}U decay chain and it diffuses in atmosphere

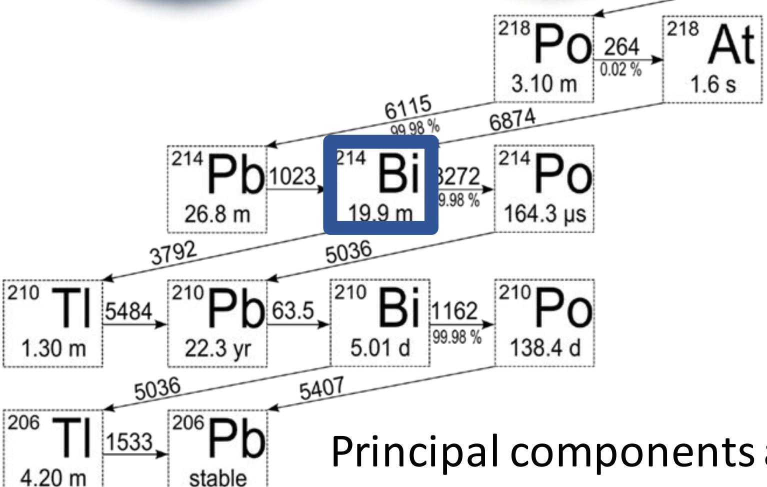

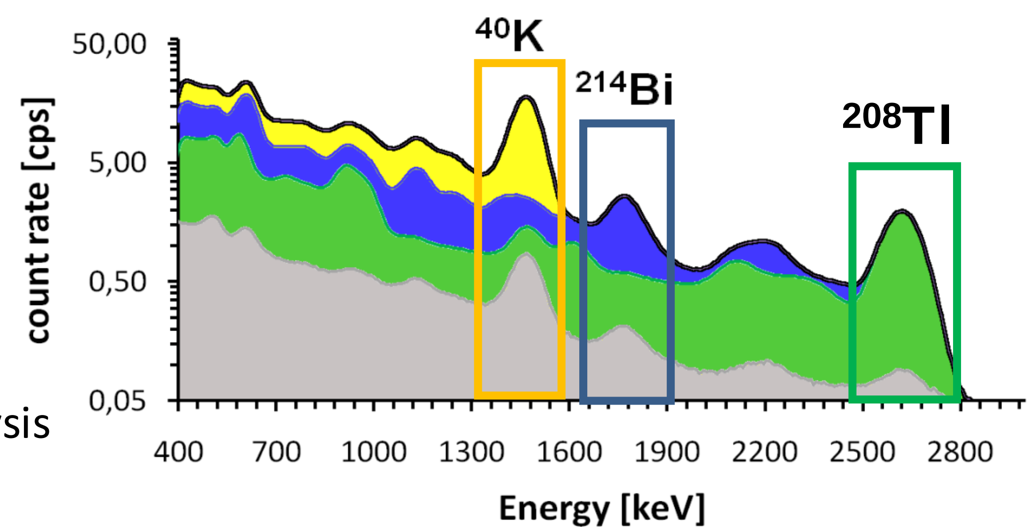

Principal components analysis in range [0.3-3.0 MeV]

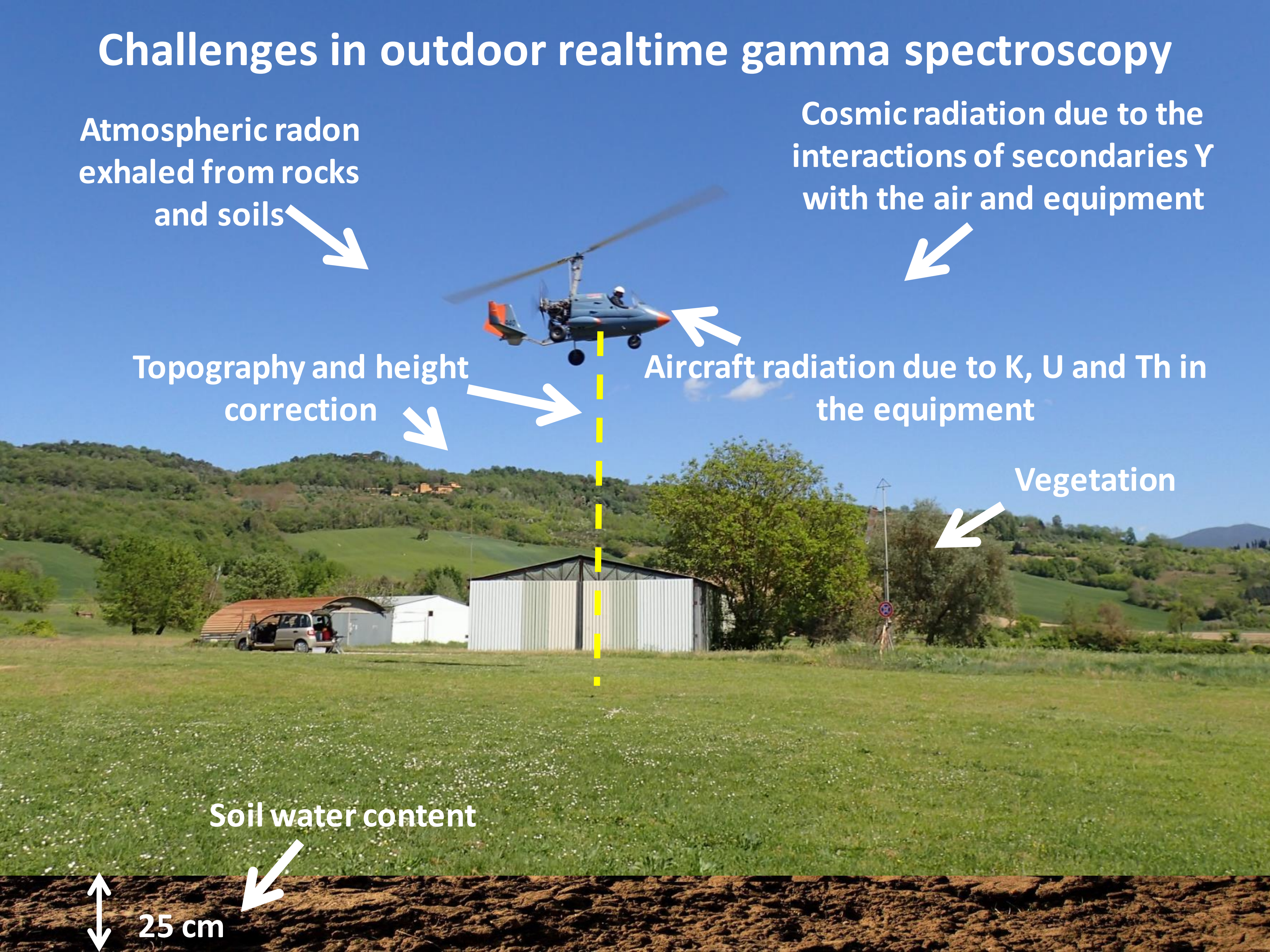
Challenges in outdoor realtime gamma spectroscopy
Atmospheric radon exhaled from rocks and soils
Cosmic radiation due to the interactions of secondaries γ with the air and equipment
Topography and height correction
Aircraft radiation due to K, U and Th in the equipment
Vegetation
Soil water content
25 cm

Scientific motivations of my PhD

Study of the accuracy of flight altitude and of its implications on the estimation of radionuclide abundances at ground level

Estimation of the airborne gamma-ray background and detection limits due to cosmic rays and aircraft radioactivity

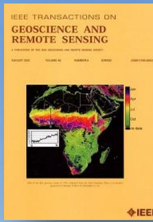

Investigation of the atmospheric radon vertical profile in a marine environment with airborne gamma-ray spectroscopy

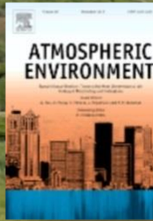

Estimation of the soil water content at an agricultural test site by means of proximal gamma-ray spectroscopy

Radgyro

The experimental autogyro devoted to airborne multiparametric measurements

Equipment on board

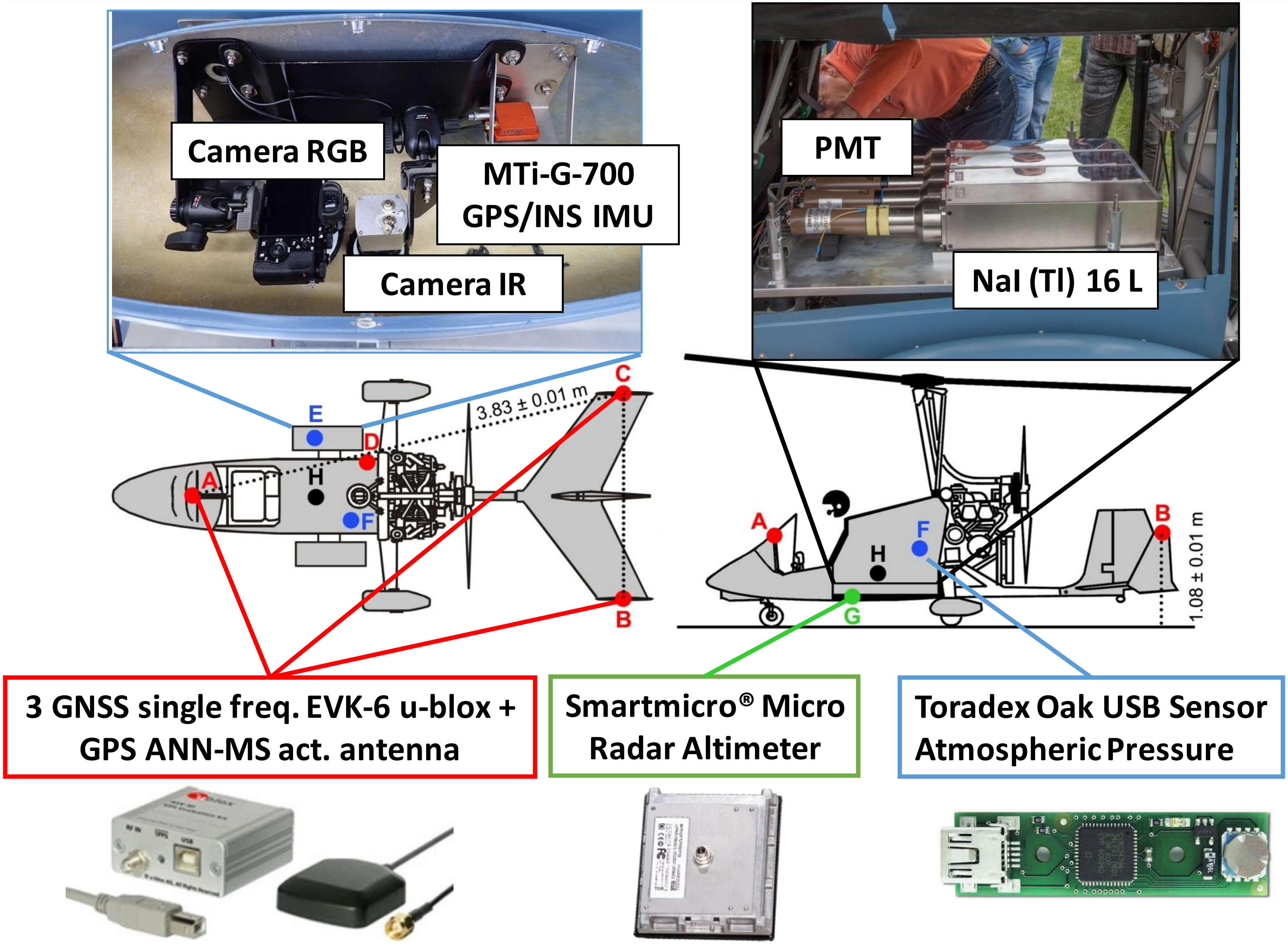

Specific surveys over the sea

- 5 different flights over the sea for avoiding the corrections of the digital elevation model (DEM) and coast's radiation
- ~ 5 hours of total data acquisition within altitude range of 35 - 3066 m collecting ~17.6 10^3 gamma spectra

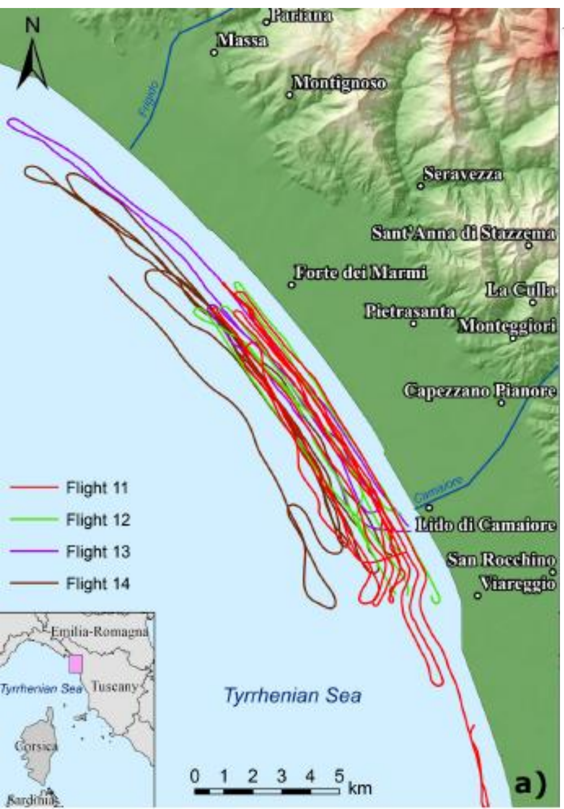

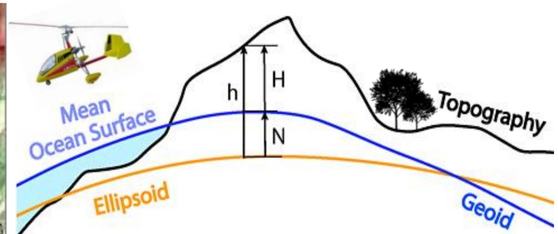

(35 – 2194) m
accuracy of flight height

(77 – 3066) m
background calibration

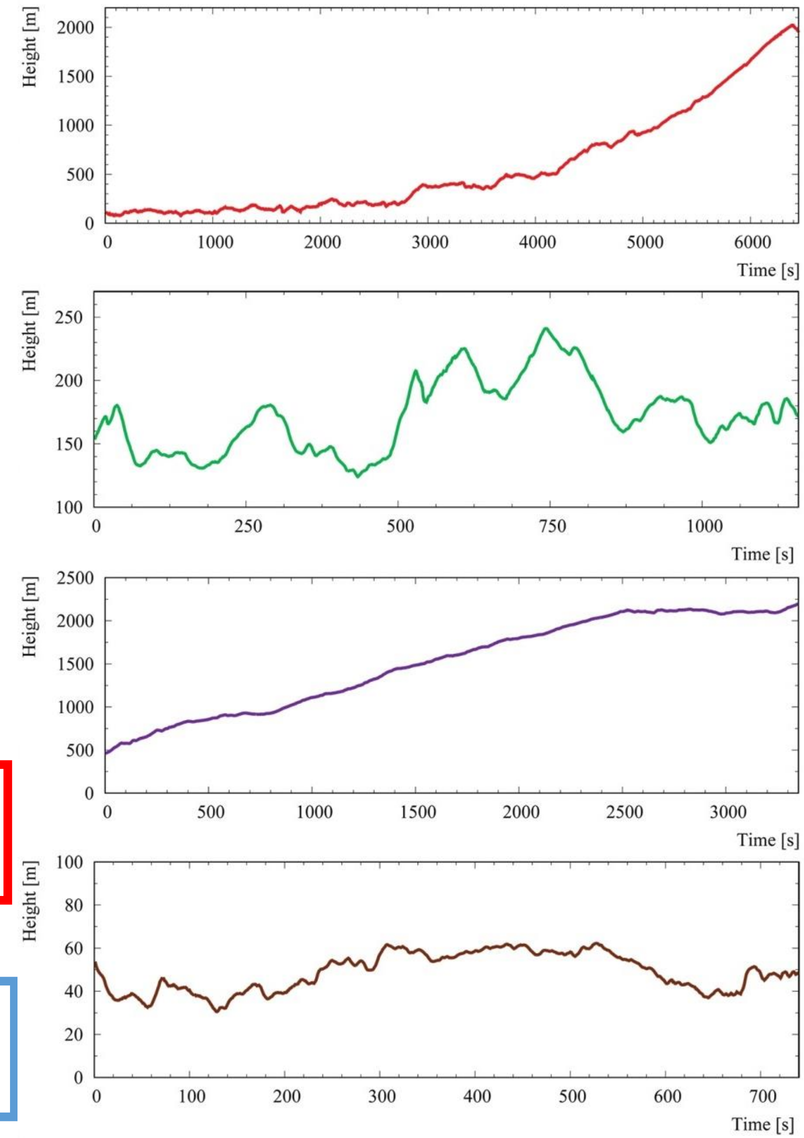

A typical pattern of heights

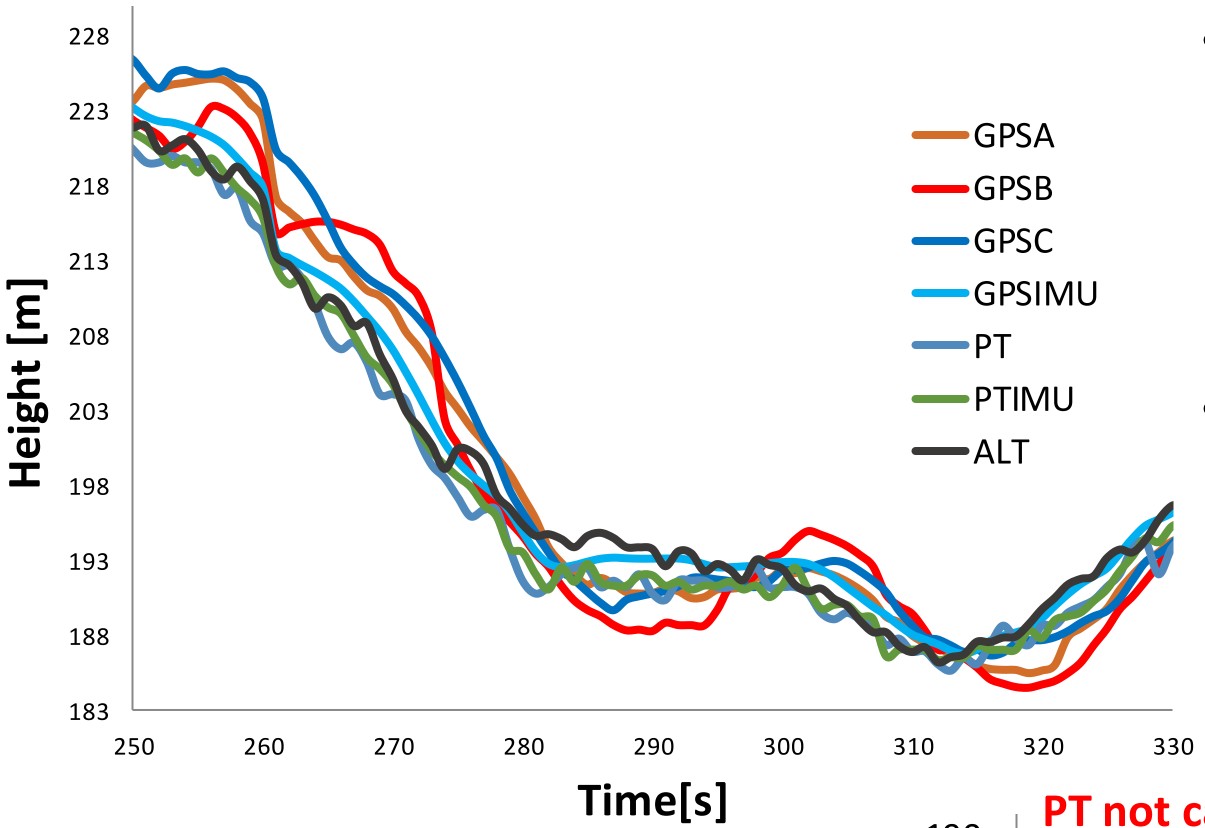

- The data acquired are time-aligned respect to the common time reference given by the PC-time stamp
- Post-processing GNSS: **code-only** and **code and phase double differences (with ground station)**

- The radar altimeter data were used in the range of 35 to 340 m
- The barometric sensors are calibrated by applying the inverse hypsometric formula averaging the heights measured by GNSS receivers and ALT

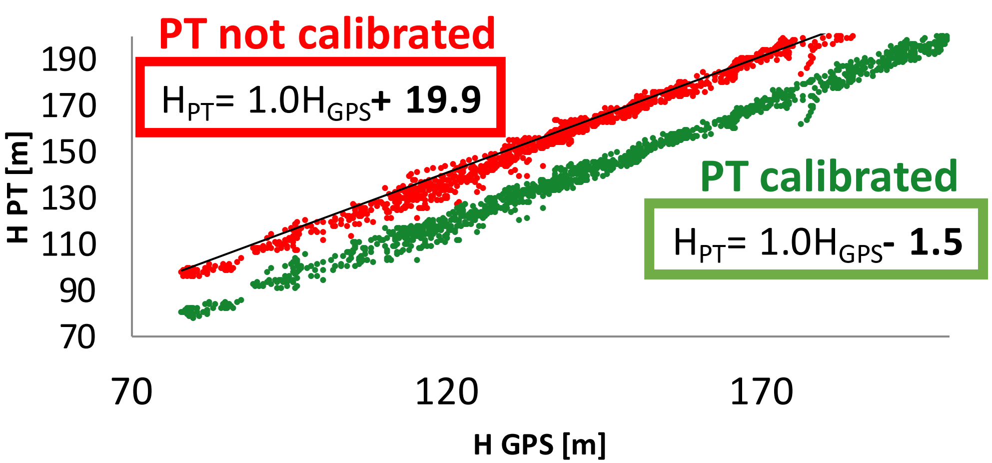

GNSS Post-processing

The identification of **outliers** performed by studying the distribution of the **distances between antennas**

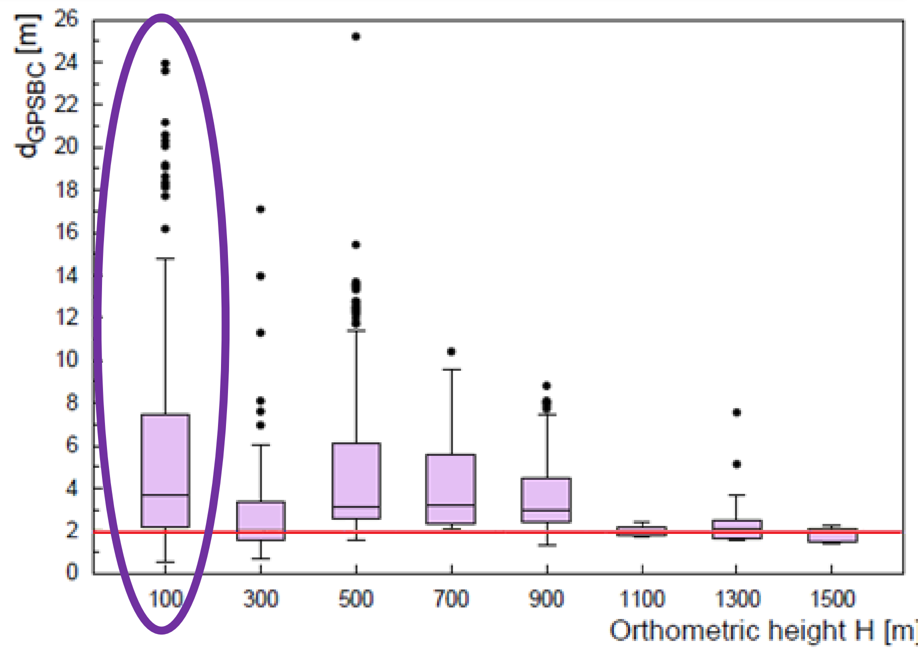

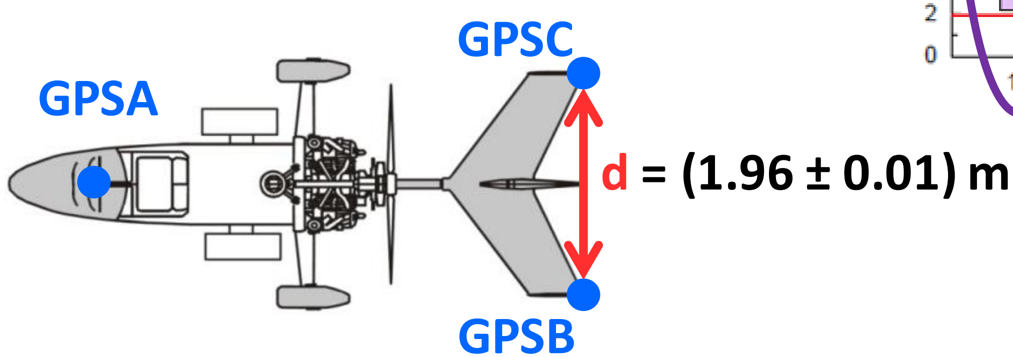

At low altitude range it is possible to observe a noise amplification due to the **multipath effect**

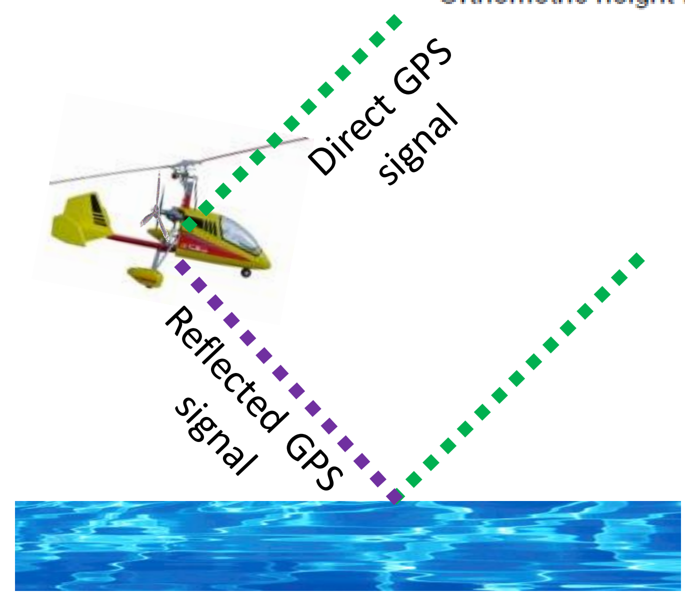

Double difference Post-processing

Distribution of σ(H) (standard deviations of heights) calculate for GPSABC **code-only post-processing (red)** and **double-difference post-processing (blue)**

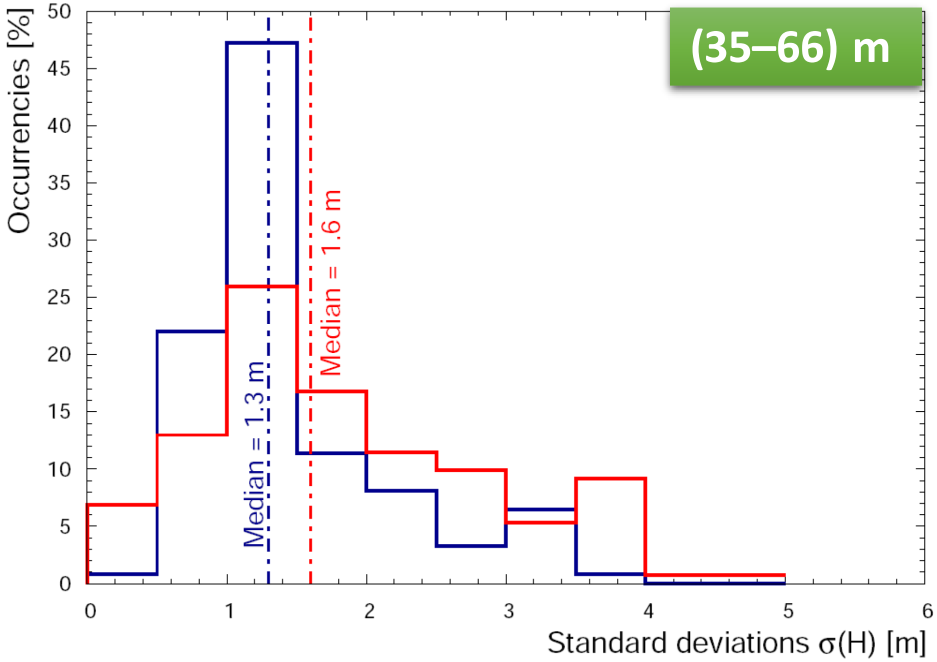

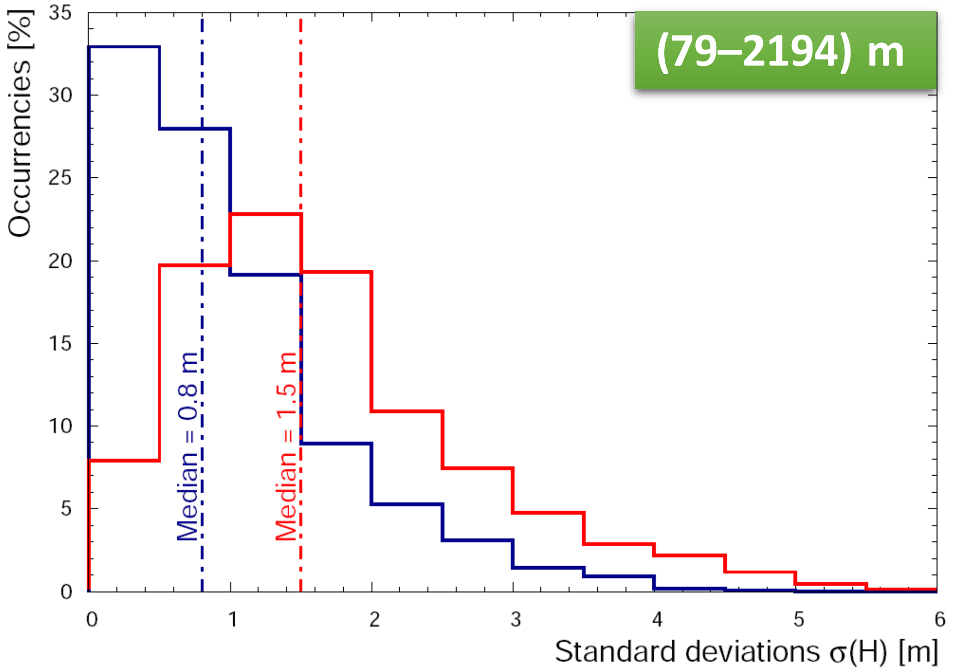

$\sigma_{GPSABC}(H) = 1.6$ m
$\sigma_{GPSABC}(H) = 1.3$ m

$\sigma_{GPSABC}(H) = 1.5$ m
$\sigma_{GPSABC}(H) = 0.8$ m

Double-difference post-processing: best results for height >79 m

Distribution of standard deviation of heights*

σ(H) with GNSS code-only post-processing

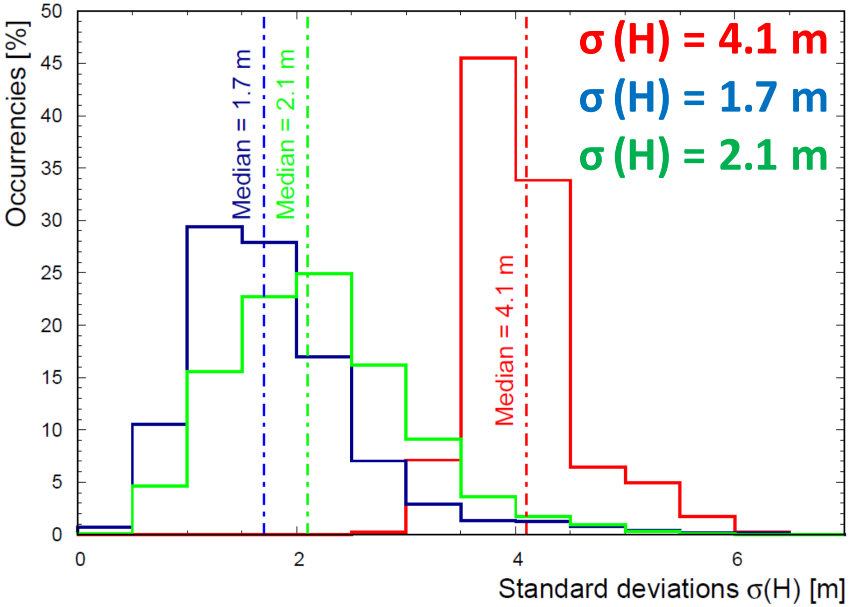

σ(H) with GNSS double-difference post-processing

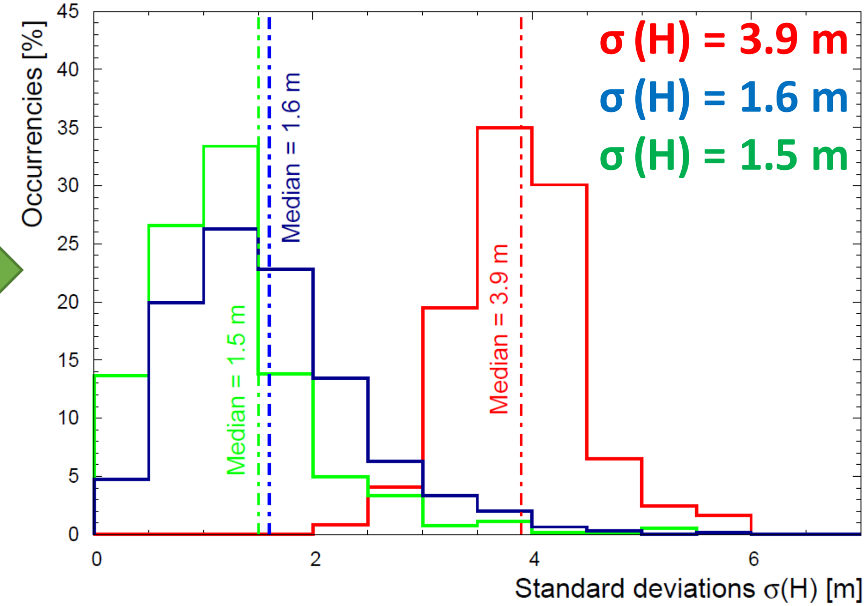

Summary of uncertainties of the flight altitude on AGRS measurements

	Height interval [m]	Estimated uncertainty on the height [m]	Relative uncertainty on the radionuclide ground abundances [%]		
			^{40}K	^{214}Bi	^{208}Tl
Low altitude	35 – 66	**3.9**	4.8	4.4	3.8
Mid altitude	79 – 340	**1.6**	1.7	1.5	1.3
High altitude	340 – 2194	**1.5**	1.6	1.4	1.2

* **Albéri M. et al. -** ***Accuracy of flight altitude measured with cheap GNSS, radar and barometer sensors: implications on airborne radiometric surveys*** **- Sensors 17(8), 1889 (2017).**

Gamma cosmic radiation

- Gamma cosmic radiation is a component of secondary cosmic rays
- **Cosmic Energy Window (CEW) (3 – 7) MeV**: gamma component of the cosmic radiation measured with AGRS
- **Tallium Energy Window (TEW) (2.4-2.8 Mev):**
- The intensity of the cosmic gamma radiation exponentially increases with the altitude

$$n(z)^{CEW} = A^{CEW} e^{\mu^{CEW} h} + B^{CEW}$$

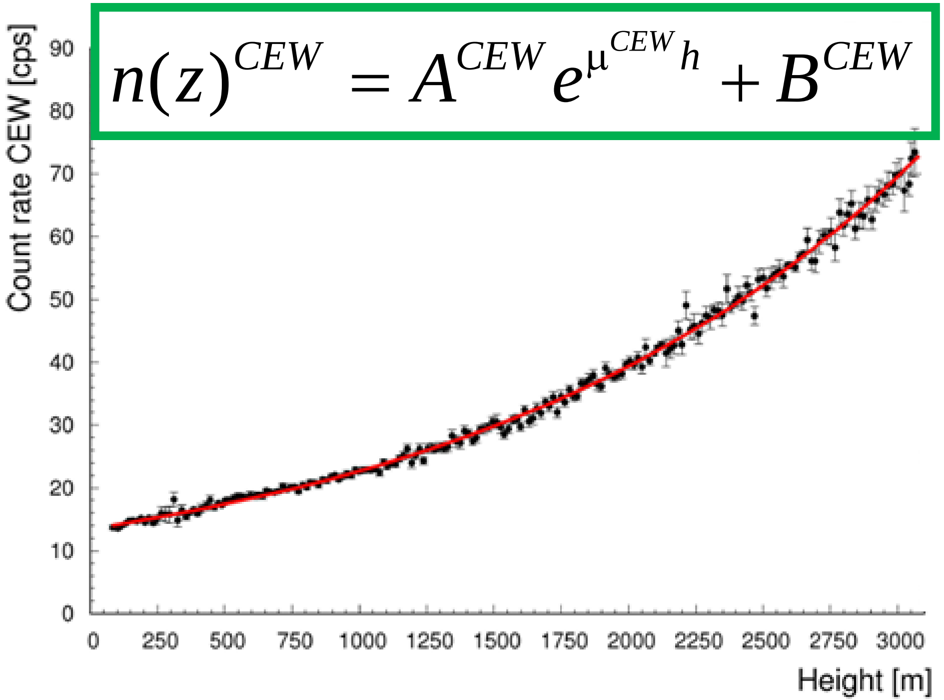

$$n(z)^{TEW} = A^{TEW} e^{\mu^{TEW} h} + B^{TEW}$$

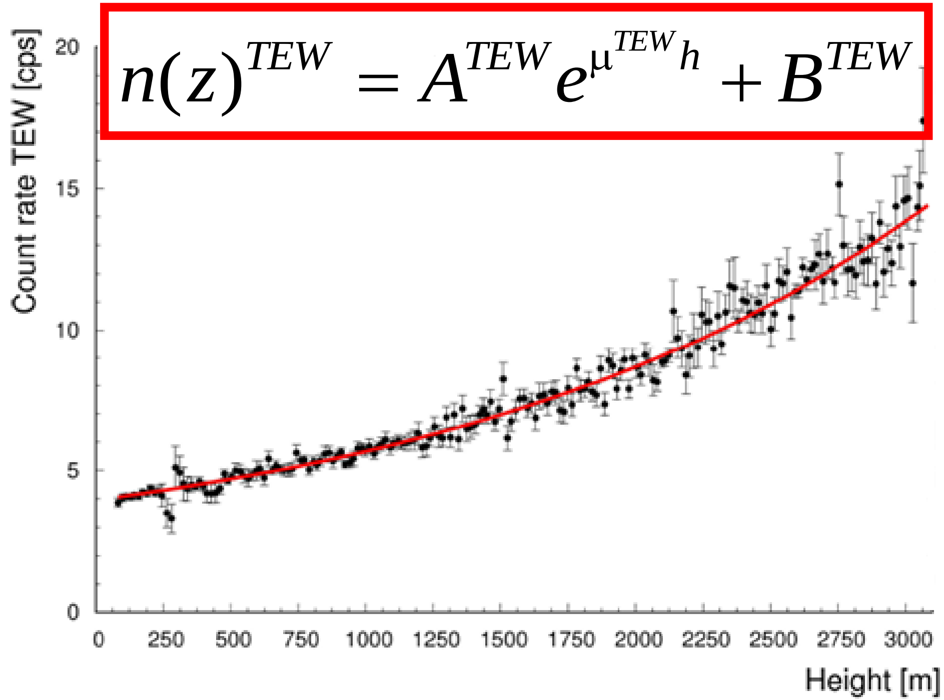

Energy Window	(A ± δA) [cps]	(μ ± δμ) [m^{-1}]	(B ± δB) [cps]	Reduced χ^2
CEW (3-7Mev)	11.4 ± 0.3	(5.9 ± 0.1) $\cdot 10^{-4}$	2.0 ± 0.4	1.12
TEW (2.4-2.8 Mev)	2.4 ± 0.2	(5.5 ± 0.2) $\cdot 10^{-4}$	1.6 ± 0.2	0.94

Cosmic spectral reconstruction

Gamma-ray spectrum composed of 870 1 second spectra acquired in the **elevation range 2050-2150 m**

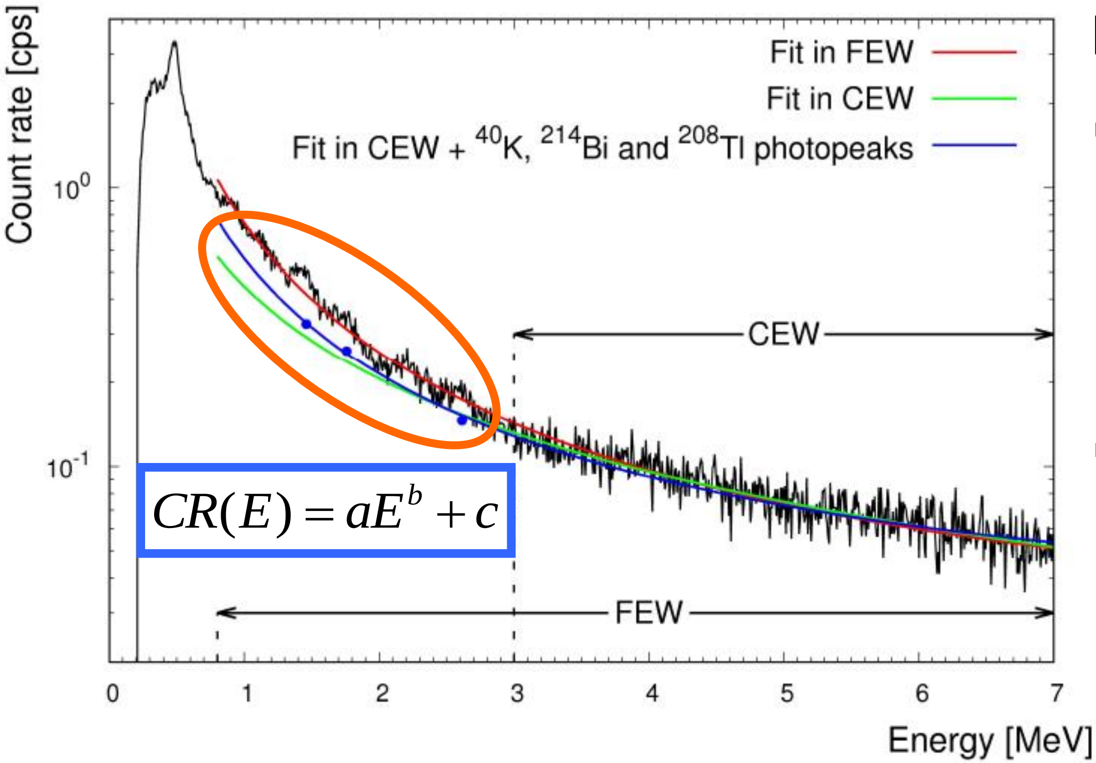

Energy Window	Photopeak energy (MeV)	Energy range (MeV)	Measured CR at 2050 - 2150 m [cps]
KEW	1.46 (^{40}K)	1.37 – 1.57	12.2
BEW	1.76 (^{214}Bi)	1.66 – 1.86	8.7
TEW	2.61 (^{208}Tl)	2.41 – 2.81	8.8
CEW	/	3.00 – 7.00	41.9

The cosmic component of a measured gamma spectrum can be reconstructed in:

- **Full Energy Windows (FEW):** the measurement contains not only the cosmic contribution to the signal, but also the **signal coming from the equipment radioactivity**
- **Cosmic Energy Window (CEW)**: the **counting statistics has pure cosmic nature** but the sole reconstruction of the high energy tail is affected by large uncertainties
- **Cosmic energy windows (CEW) + ^{40}K + ^{214}Bi + ^{208}Tl photopeaks** aid **constraining the low energy** trend of the cosmic shape, necessary to separate the K, U and Th **constant aircraft and instrument component**

Cosmic Background and Minimum Detection Aboundance (MDA)

The CR in the natural radionuclides energy windows are linearly related to the count rate in the CEW

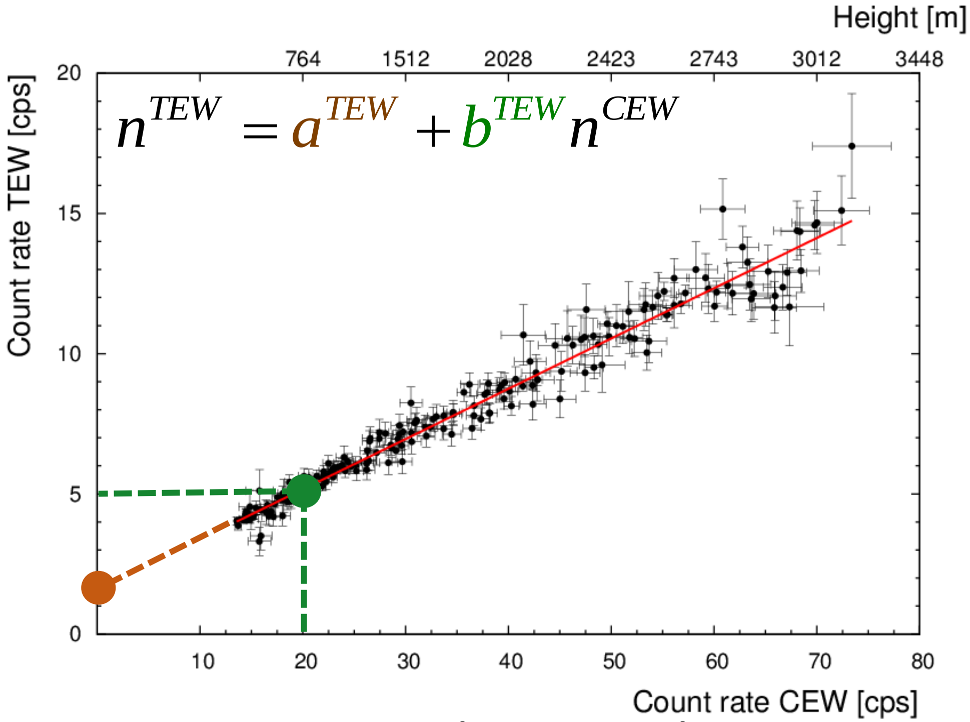

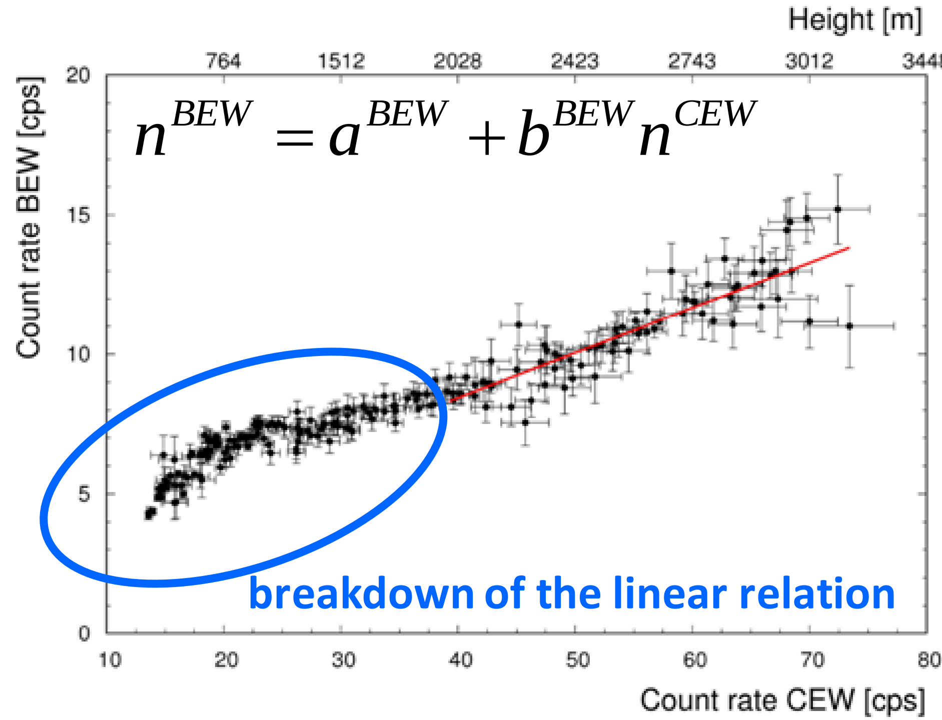

Linear regressions between the count rates in KEW BEW TEW and CEW allows to **correct the CRs measured at a given height** during regional AGRS surveys

b: cosmic stripping ratio

a: aircraft constant background count rate

Energy Window	(a ± δa) [cps]	MDA	(b ± δb) [cps/cps in CEW]	Reduced χ2
KEW	3.7 ± 0.4	$0.05 \cdot 10^{-2}$ g/g	0.20 ± 0.01	1.00
BEW	2.0 ± 0.4	0.4 μg/g	0.16 ± 0.01	1.02
TEW	1.58 ± 0.04	0.8 μg/g	0.179 ± 0.002	1.02

A new model for count rate in BEW

- In presence of atmospheric radon, **the CR in BEW comprises an altitude dependent component coming from atmospheric ^{214}Bi (Rn):**

$$n(z) = A_{BEW} e^{\mu^{BEW} h} + B_{BEW} + n_{Rn}$$

- Recent studies of ^{222}Rn vertical profile applied to climate, air quality and pollution showed a **diurnal mixing layer at ~ 1-2 km**

- We aimed to develop a real-time method for recognizing the ^{222}Rn boundary layer with AGRS measurements, taking into account **2.3 mean free path (r ~ 400 m) of ^{214}Bi** unscattered photon

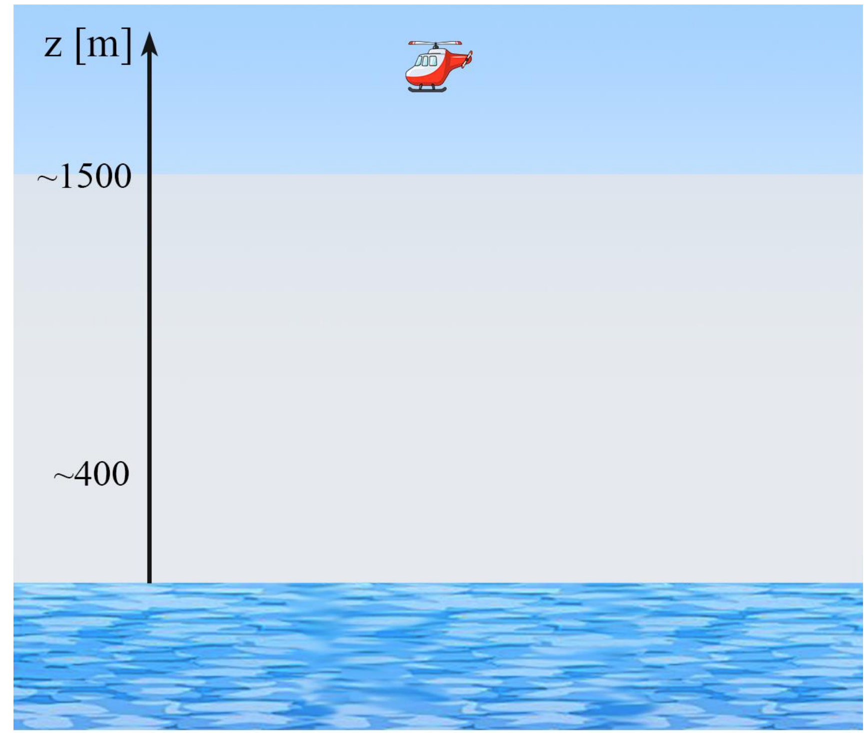

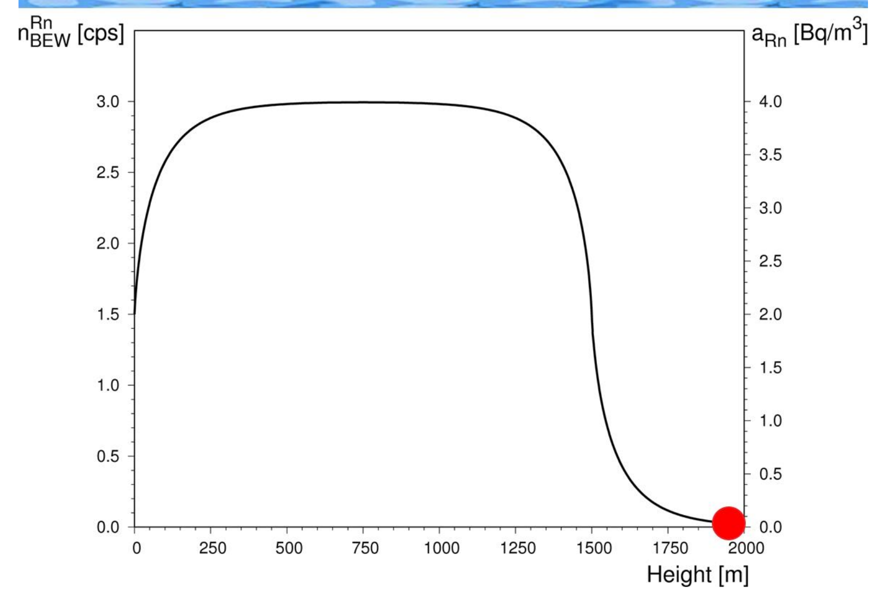

Fit of AGRS measurement

The theoretical model is applied for fitting the experimental count rate in BEW

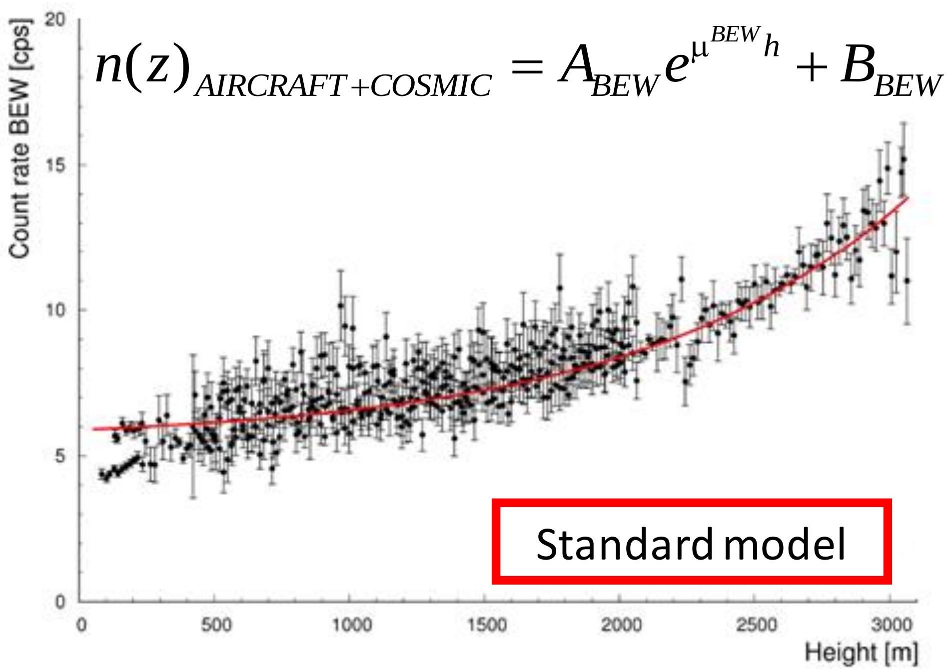

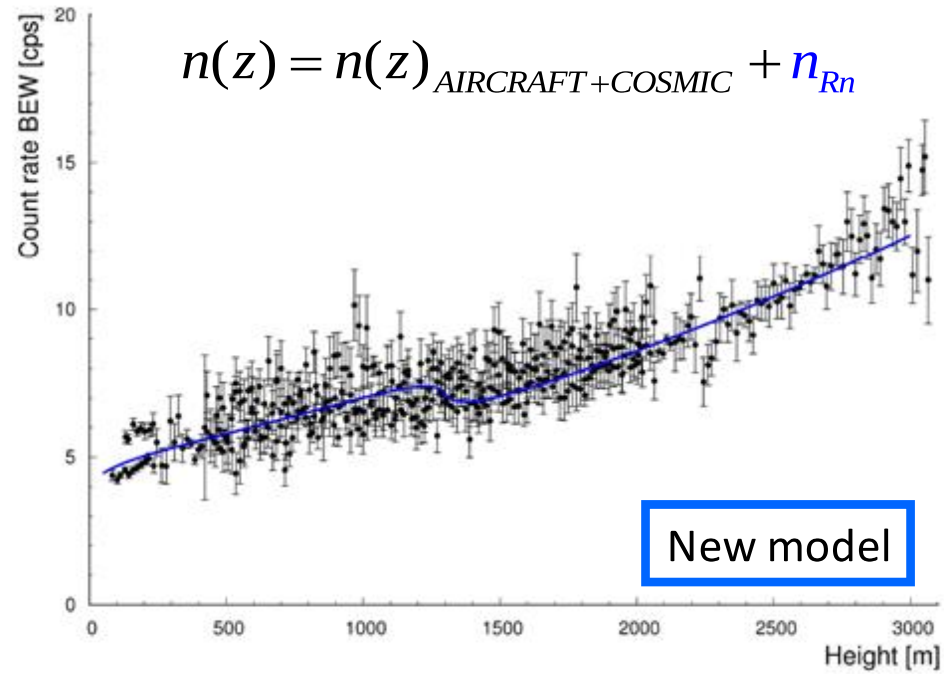

Theoretical model	$A_{BEW} \pm \delta A_{BEW}$ [cps]	$\mu_{BEW} \pm \delta\mu_{BEW}$ [m^{-1}]	$B_{BEW} \pm \delta B_{BEW}$ [cps]	$s \pm \delta s$ [m]	$C \pm \delta C$ [cps]	Reduced χ^2
Standard model	0.39 ± 0.07	$(2.01 \pm 0.1) \cdot 10^{-3}$	5.5 ± 0.3	/	/	**5.0**
New model	8.2 ± 0.2	$(2.54 \pm 0.06) \cdot 10^{-4}$	-4.9 ± 0.2	1318 ± 22	0.68 ± 0.05	**2.1**

Concentration of Rn=(0.96 ± 0.07) Bq/m^3 distribuited up to (1318 ± 22) m

- The **new model** fits the data better than the **standard model**
- The mean ^{222}Rn concentration and mixing layer depth are in agreement with the literature : **a_{Rn} ~ 1 Bq/m^3, s ~ 1500 m**

…since the water shields gamma ray from the Earth… why don’t use the gamma spectrometry for measuring the soil water content in precision agriculture?

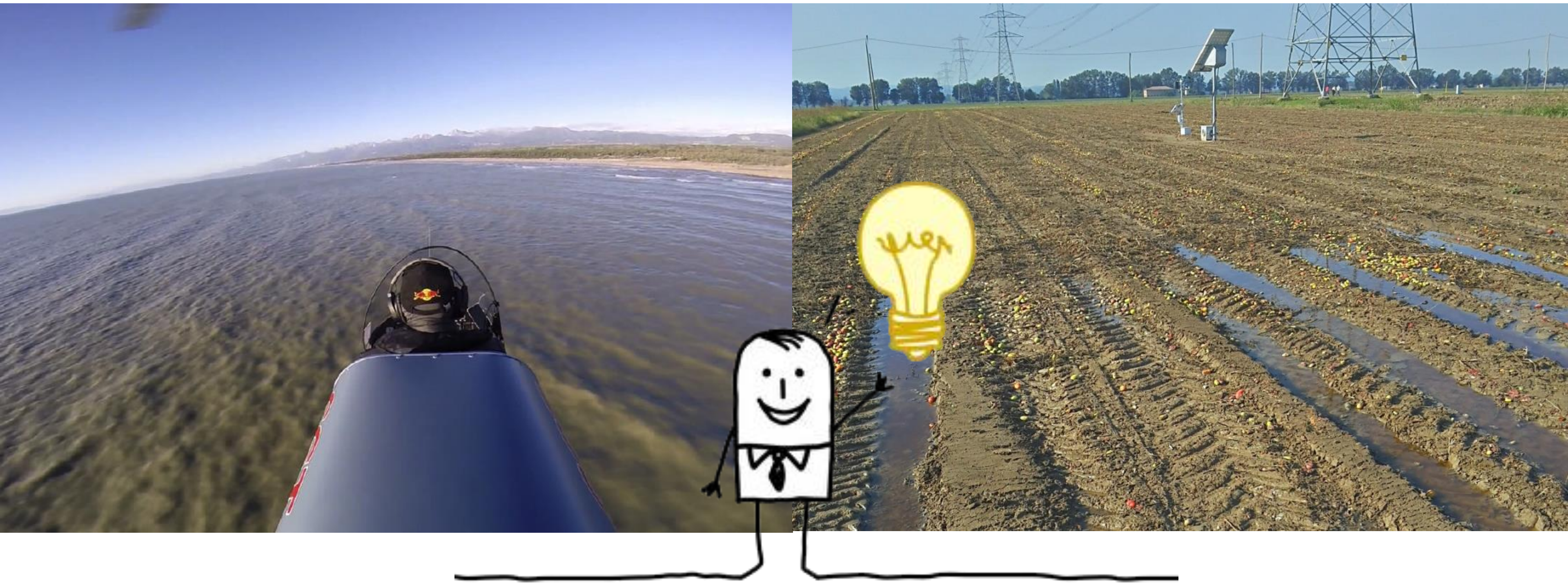

The soil water content θ is inversely proportional to the signal S (K) produced by the ^{40}K decay measured by the gamma spectrometer

$$\theta = \frac{33.6}{S(K)} - 1.20$$

Regional project supported by POR FESR funds

ALADIN AgroAlimentare IdroIntelligente

Gamma spectroscopy applied to precision agriculture

GOAL: study the soil water content measuring the attenuation effects on gamma rays emitted by terrestrial radionuclides during a tomato crop season

Experimental site

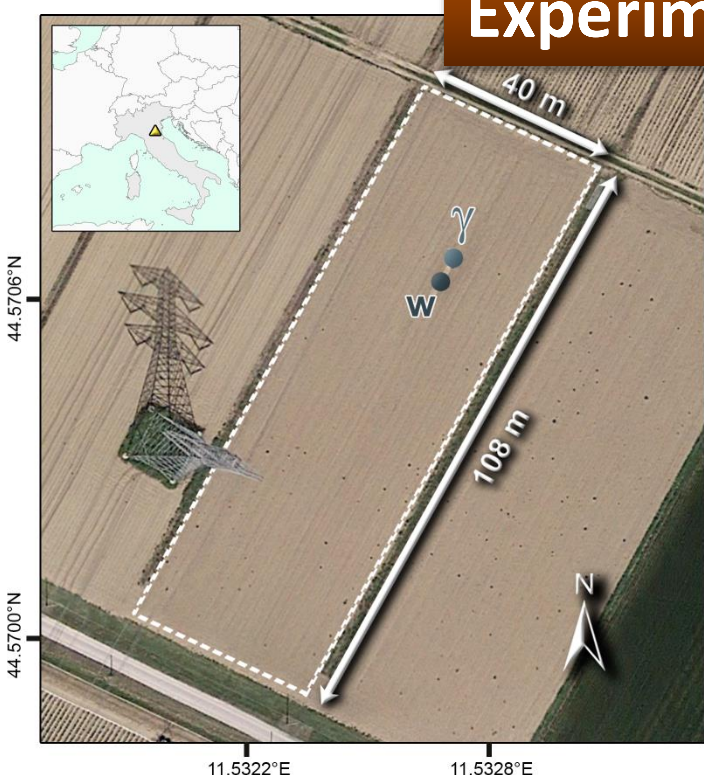

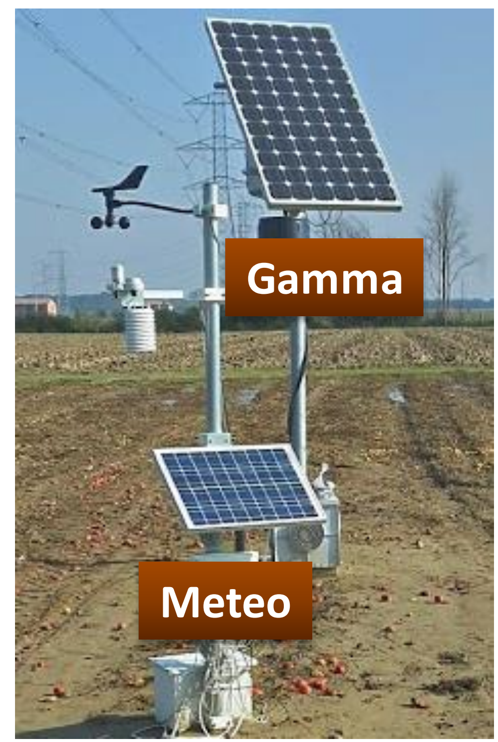

The equipment

Agrometeorological station (M)
Thermo-hygrometer, solar pyranometer, ultraviolet radiation, anemometer, rain collector, digital barometer, GPRS connection, storage on sd card
Gamma station (Y)
1L sodium iodide scintillator NaI (Tl) at 2.3 m height, CAEN Gamma Stream multichannel analyzer, 3 G connection, list-mode acquisition, storage on sd card

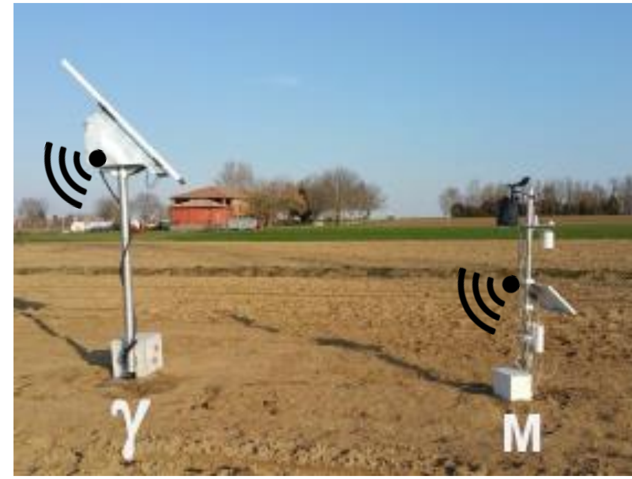

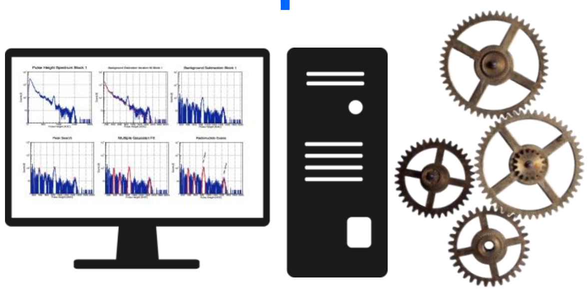

- Production of spectra with a 15 minutes of acquisition time
- Energy autocalibration
- CPS and radionuclide abundances
- Meteo and gamma time alignment

Data taking: 04/04/2017 - 02/11/2017
Duty cycle: 95.4%
Raw data: 260 GB
Temporal resolution: 15 minutes
Total number of output: 44
Total entries: 20502

Gamma station: vertical and horizontal field of view

In a typical soil ~ 95% of the gamma radiation is emitted from the top 25 cm of the soil

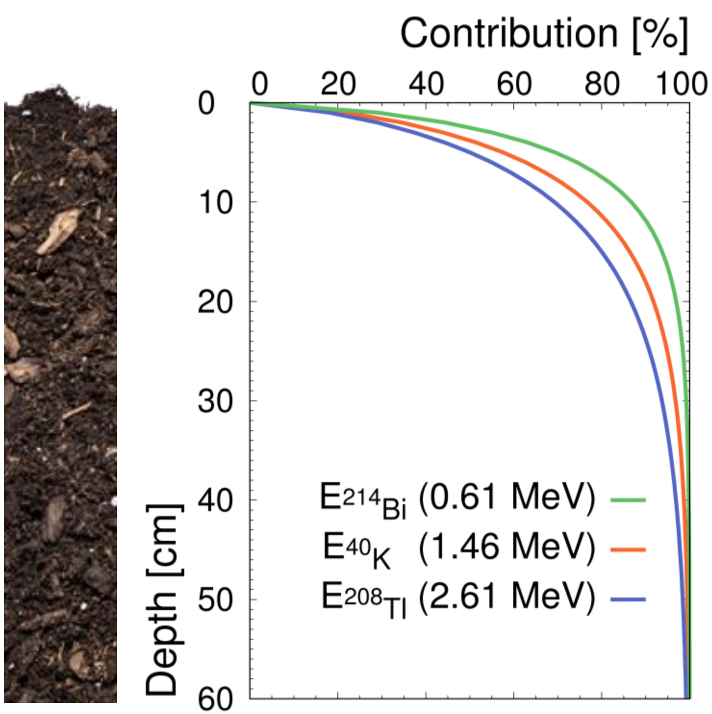

Cumulative contribution of ground radioactivity in percentage as function of the source radius detected at height of 2.3 m reaches ~ 95% at ~ 25 m of radius

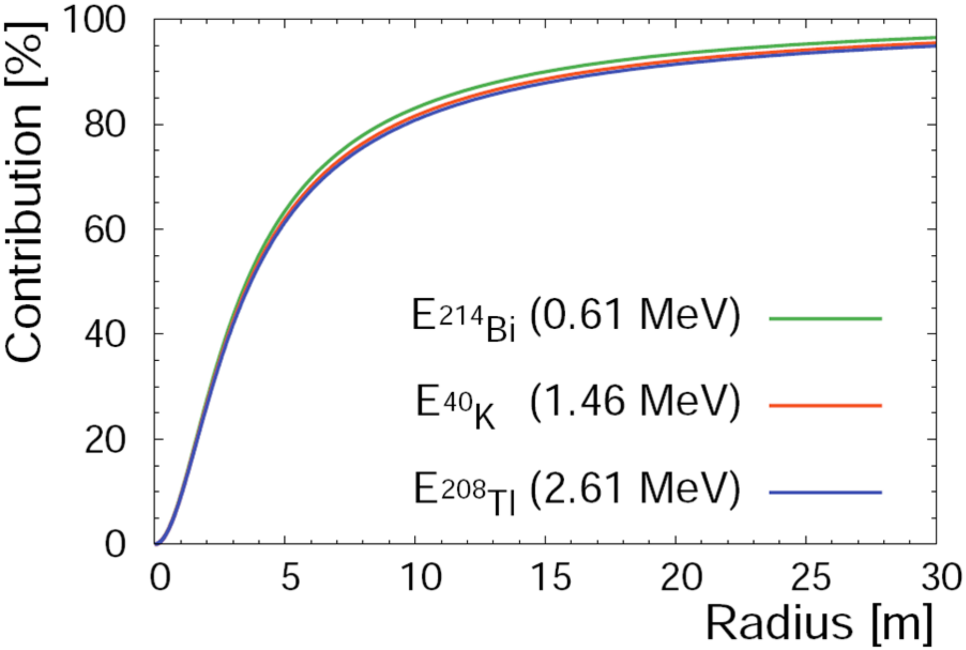

Experimental site spectrum

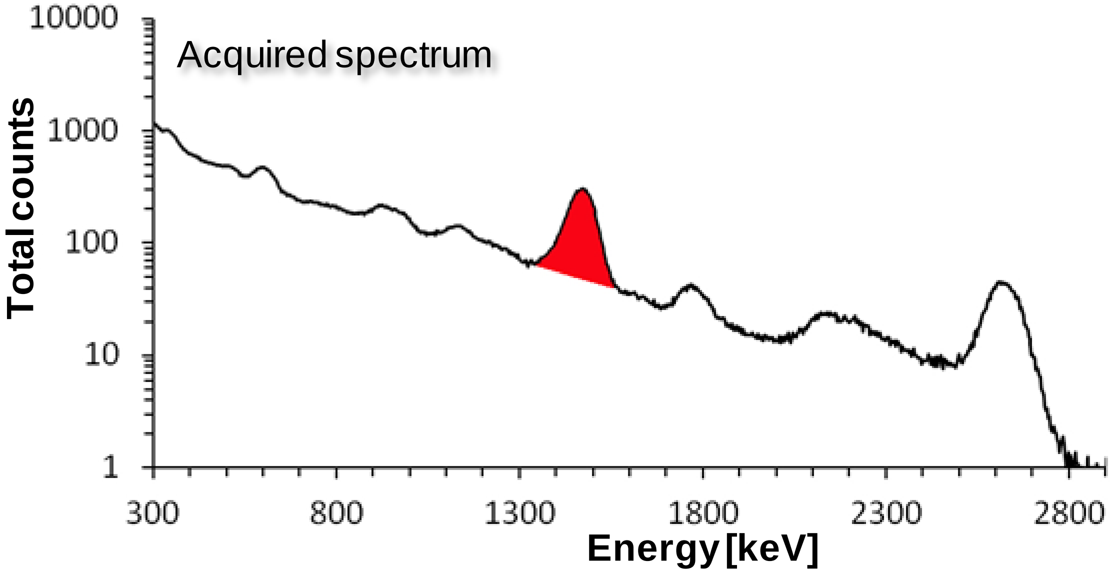

- 10 minutes acquired spectrum
- Total counts ~ 120 10^3
- Net counts in ^{40}K window ~ 6 10^3
- Statistical noise of ~ 0.5 % for 1h acquisition

Soil chemical characteristics			
OX	%	El.	Abb.
SiO_2	55.7± 0.6	K	1.61 ± 0.16 %
Al_2O_3	11.7±0.1	Th	9.47 ± 1.08 ppm
CaO	9.6±0.1	U	2.51 ± 0.25 ppm

Knowing the chemical composition of the soil and the water content, **Monte Carlo (MC) simulation** allows to reconstruct the entire gamma spectrum

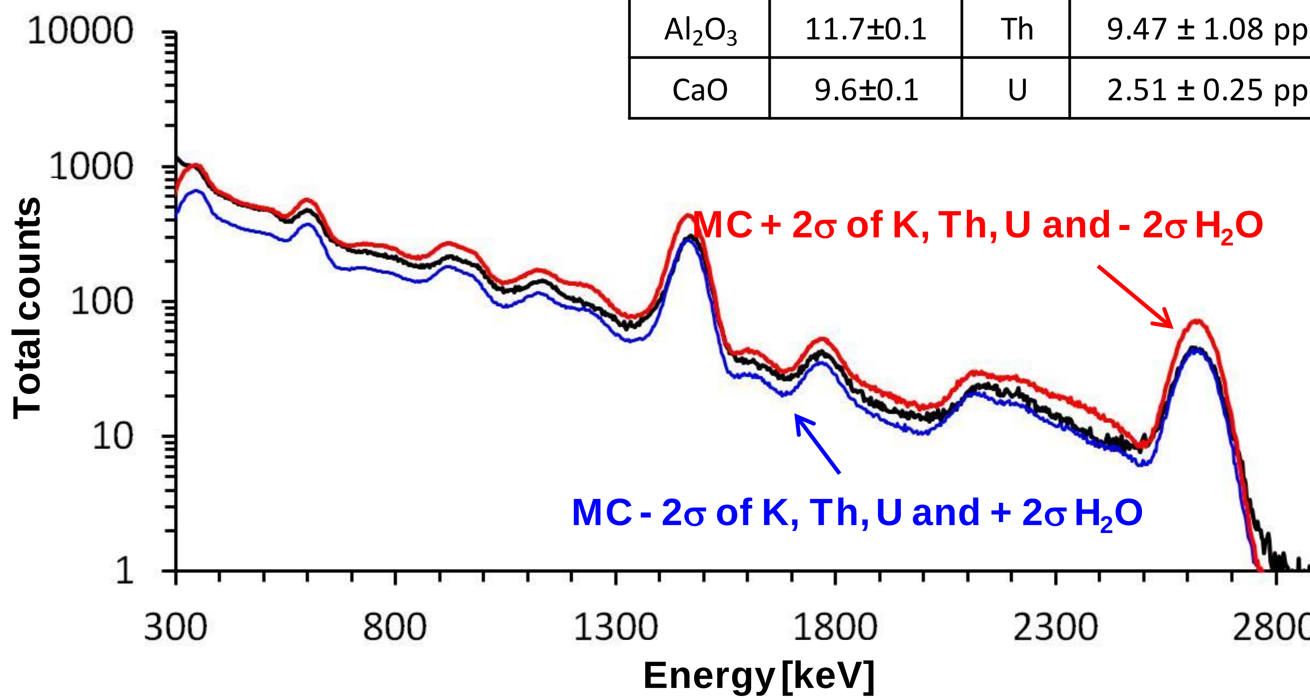

Calibrations procedure

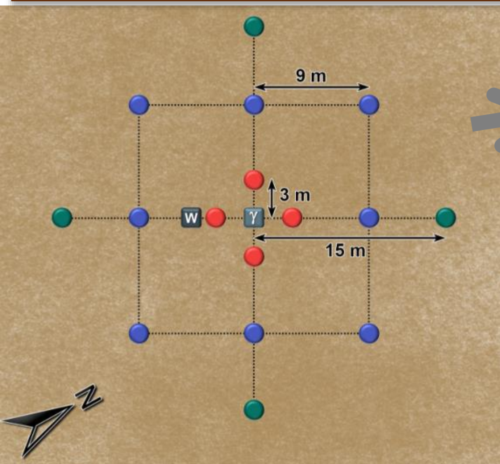

On 18 Sept. 2017, 16 samples collected at different distance the gravimetric water content w_{CAL} was measured

$$w_t[\frac{kg}{kg}] = \frac{CR_{CAL}[cps]}{CR_i[cps]}(0.899 + w_{CAL}) - 0.899$$

The gravimetric water content w at time t inferred by K counts rates is obtained after setting the calibration data: gravimetric water content (w_{CAL}) and count rate in ^{40}K window (CR_{CAL})

$$\theta[\frac{m^3}{m^3}] = \frac{V_{water}}{V_{dry\ soil}} = w \times \frac{\rho_{dry\ soil}}{\rho_{water}}$$

From the count rates to the water content in soil

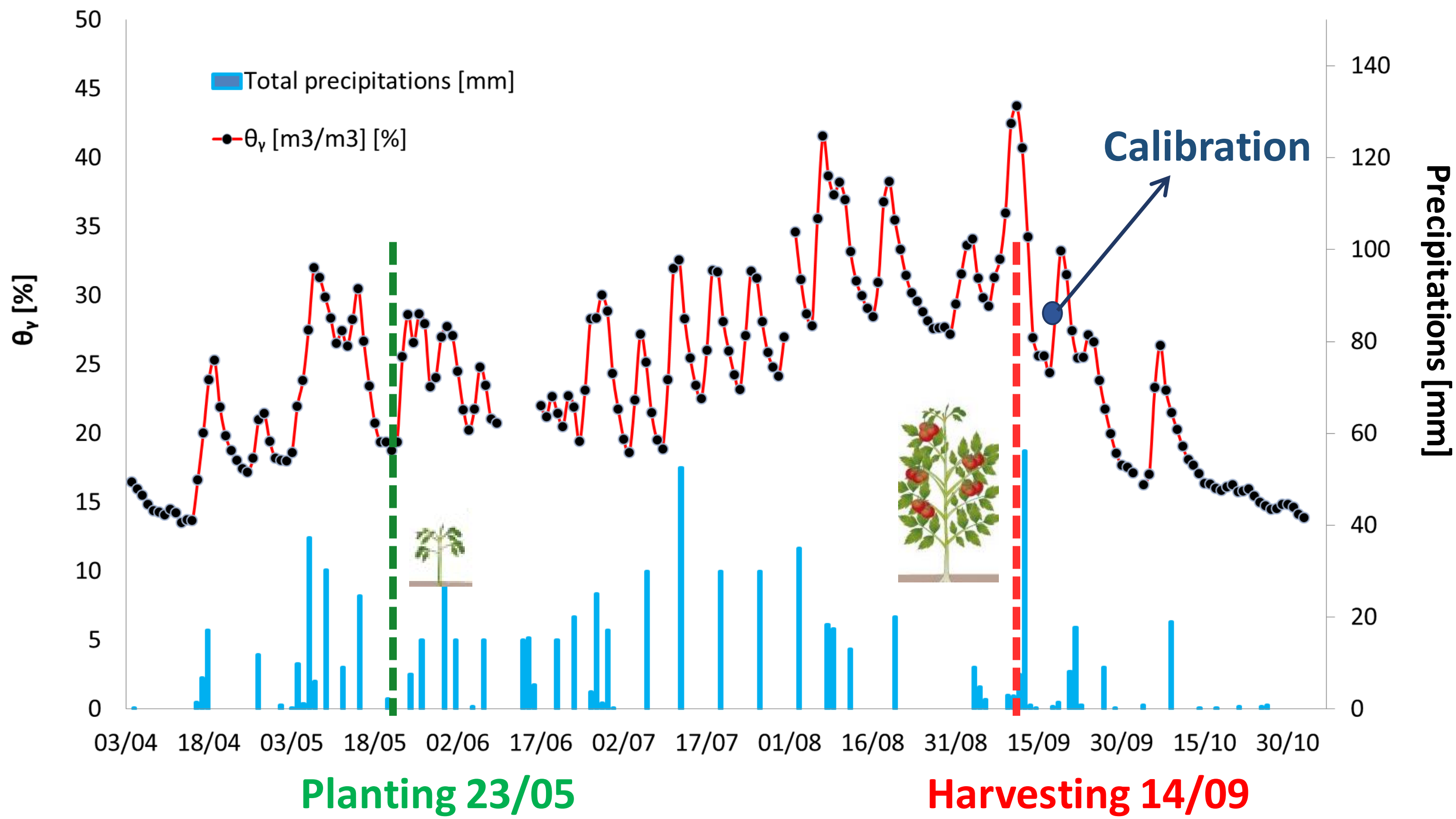

- Daily measurements of the water content θ_γ on the basis of **the gravimetric calibration measures of 18/9/2017 (taken in bare soil condition)**
- Excellent sensitivity to changes in θ_γ due to rainfall and irrigation is observed

Comparison with gravimetric measurements

Bare soil			
Date	θ_G [m³/m³]	θ_γ [m³/m³]	$\Delta\theta$
21/09/17	23.7 ± 1.5	24.5 ± 1.1	3.4 %
Calibration Day			
18/09/17	21.9 ± 1.0	21.9 ± 2.8	0.0 %

With plants			
Date	θ_G [m³/m³]	θ_γ [m³/m³]	$\Delta\theta$
24/07/17	16.7 ± 2.8	26.3 ± 2.0	57.5 %
26/07/17	26.5 ± 2.8	34.4 ± 1.4	30.0 %
28/07/17	18.9 ± 1.5	27.3 ± 0.4	43.9 %

- The values of water contents estimated via gamma and via gravimetric measurements are in **perfect agreement in bare soil condition**
- When the **soil is covered by tomato plants** the gamma signal decreases consequently **the estimated water content increases**: this is an evidence of “shielding effect”.

Estimating plants shielding effect with Monte Carlo simulation

A tomato plant consists of about 90% of water

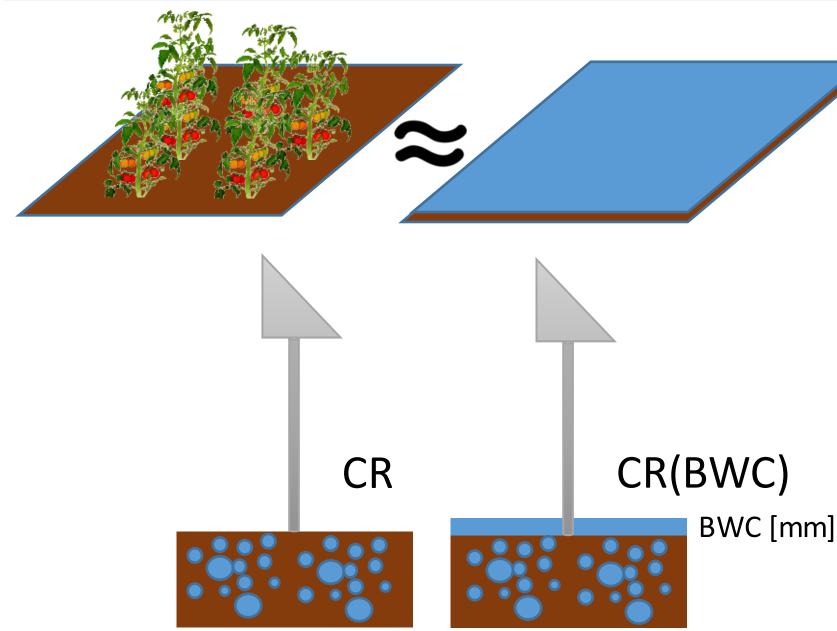

- The vegetative cover produces a **shielding effect** and then an overestimation of water content.
- The plants can be approximated to a layer of water that corresponds to the **biomass water content (BWC)** in kg/m^2 (numerically equal to the water height in mm)
- The count rate attenuation produced by the BWC is given by:

$$\Lambda = \frac{CR(BWC[mm])}{CR}$$

$$w_i = \frac{CR_{CAL}}{CR_i}\boxed{\Lambda_i}(0.899 + w_{CAL}) - 0.899$$

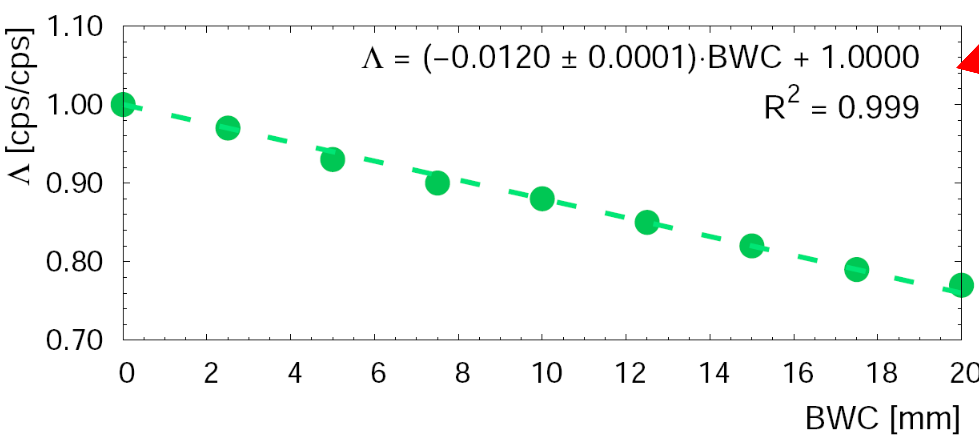

MC simulation allows to estimate the effect of attenuation as a function of the BWC

Shielding estimation from BWC measurements

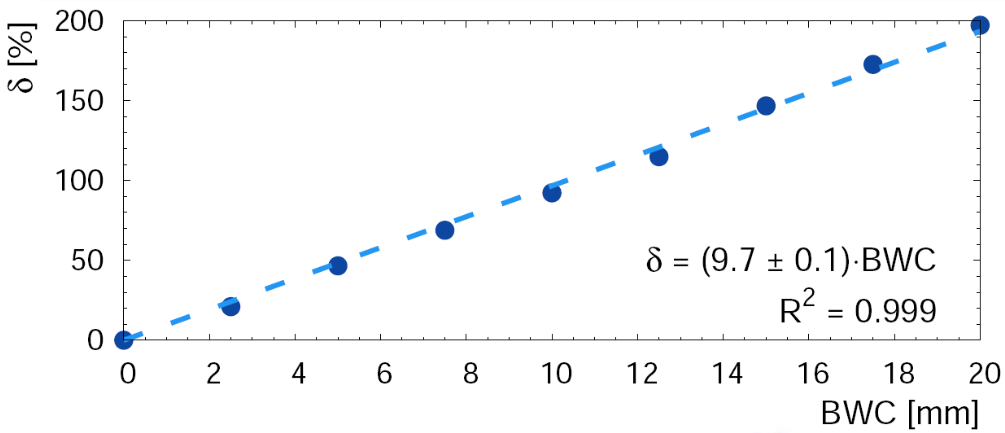

5 mm of water homogenously distributed produces an overestimation of 50% of the water content in the soil

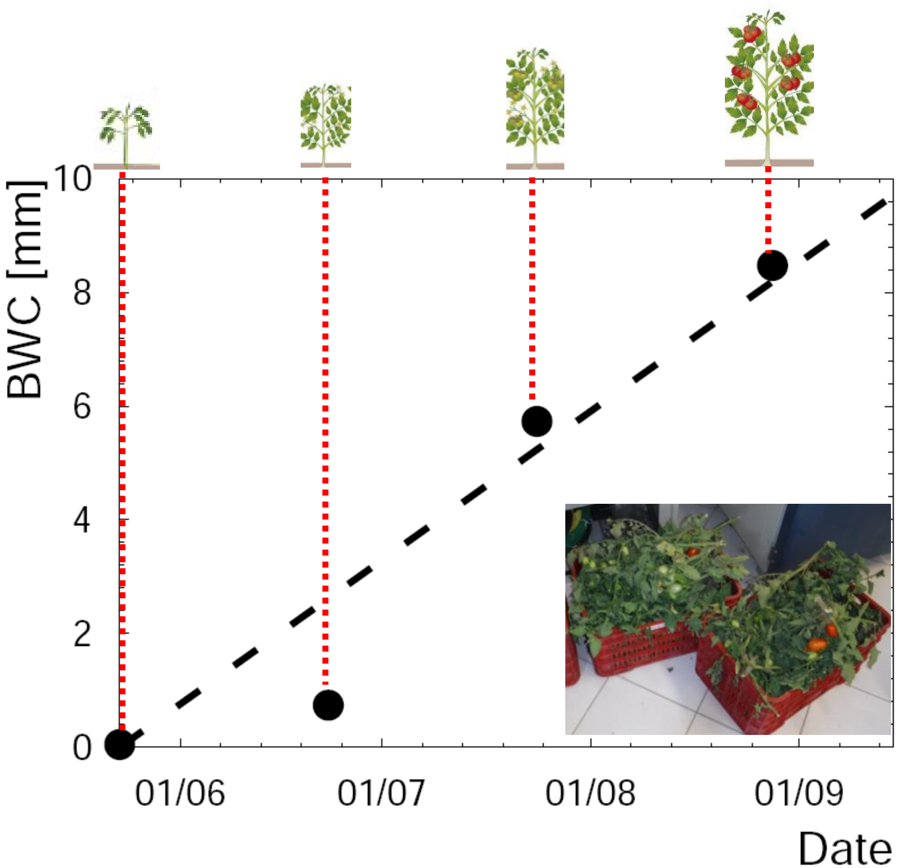

- The water content in tomato plants was estimated from destructive above-ground biomass samples at different stages of plant growth
- A straight line function was calculated for describing the growth of BWC in time:

$$BWC[mm] = 3.5 \cdot 10^{-3} \times t[h]$$

Results

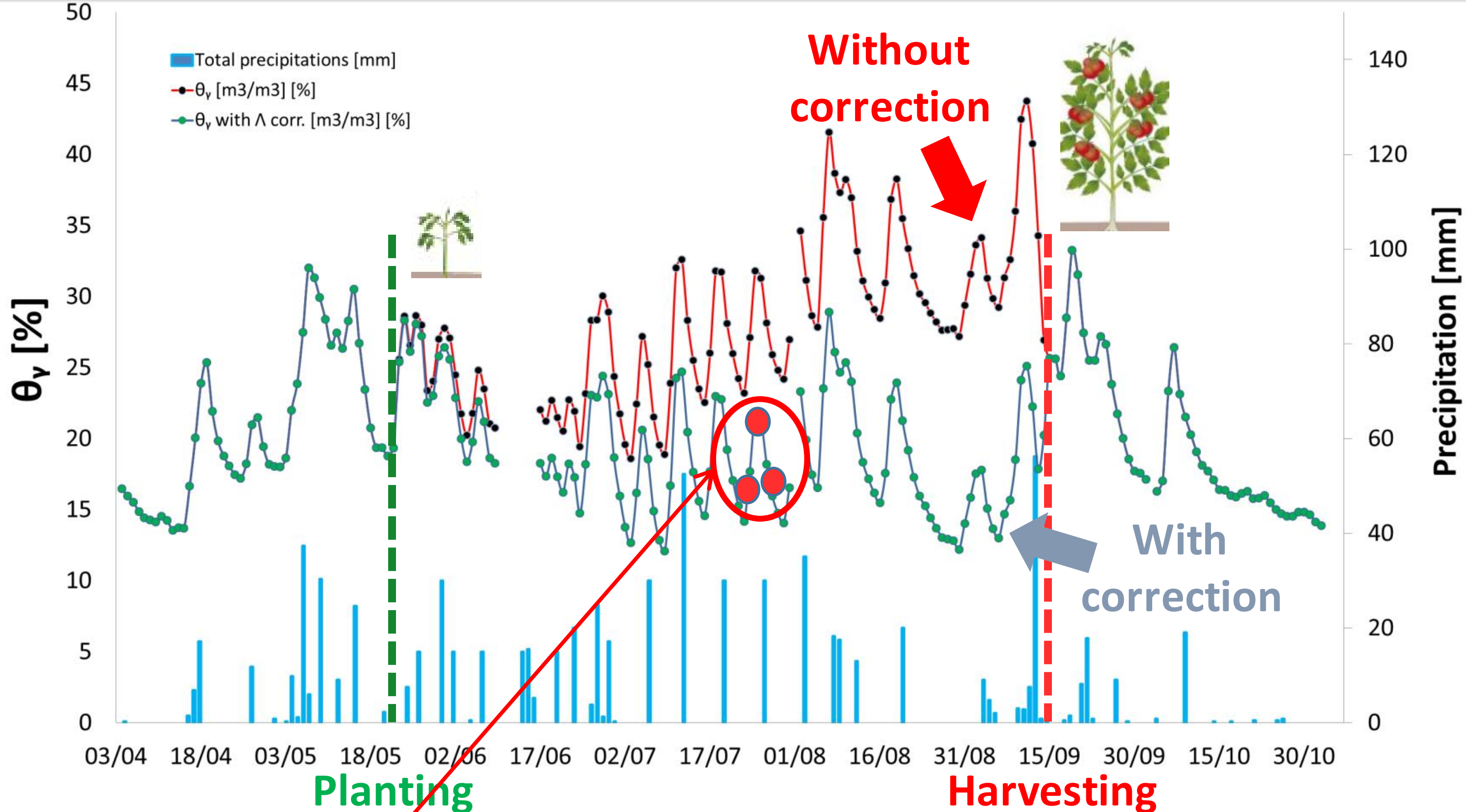

	With Λ(BWC) correction		
Date	θ_G [m³/m³]	θ_γ [m³/m³]	Δθ
24/07/17	16.7 ± 2.8	17. 0 ± 1.9	1.8 %
26/07/17	26.5 ± 2.8	24.3 ± 1.3	-8.3 %
28/07/17	18.9 ± 1.5	17.9 ± 1.5	-5.7 %

The correction introduced by Λ function is effective:
The soil water contents θ_γ are compatible at 1σ level with gravimetric field measurements θ_G with a maximum difference between the central values of 8.3%

Corroborating hydrological models and gamma ray measurements

- **CRITeRIA** is a **physically-based numerical model** for simulating soil water balance
- **AquaCrop** is the FAO **conceptual-based model** for water management effects on crop production

Requirements:
- Soil parametrization
- Crop parametrization
- Meteo data

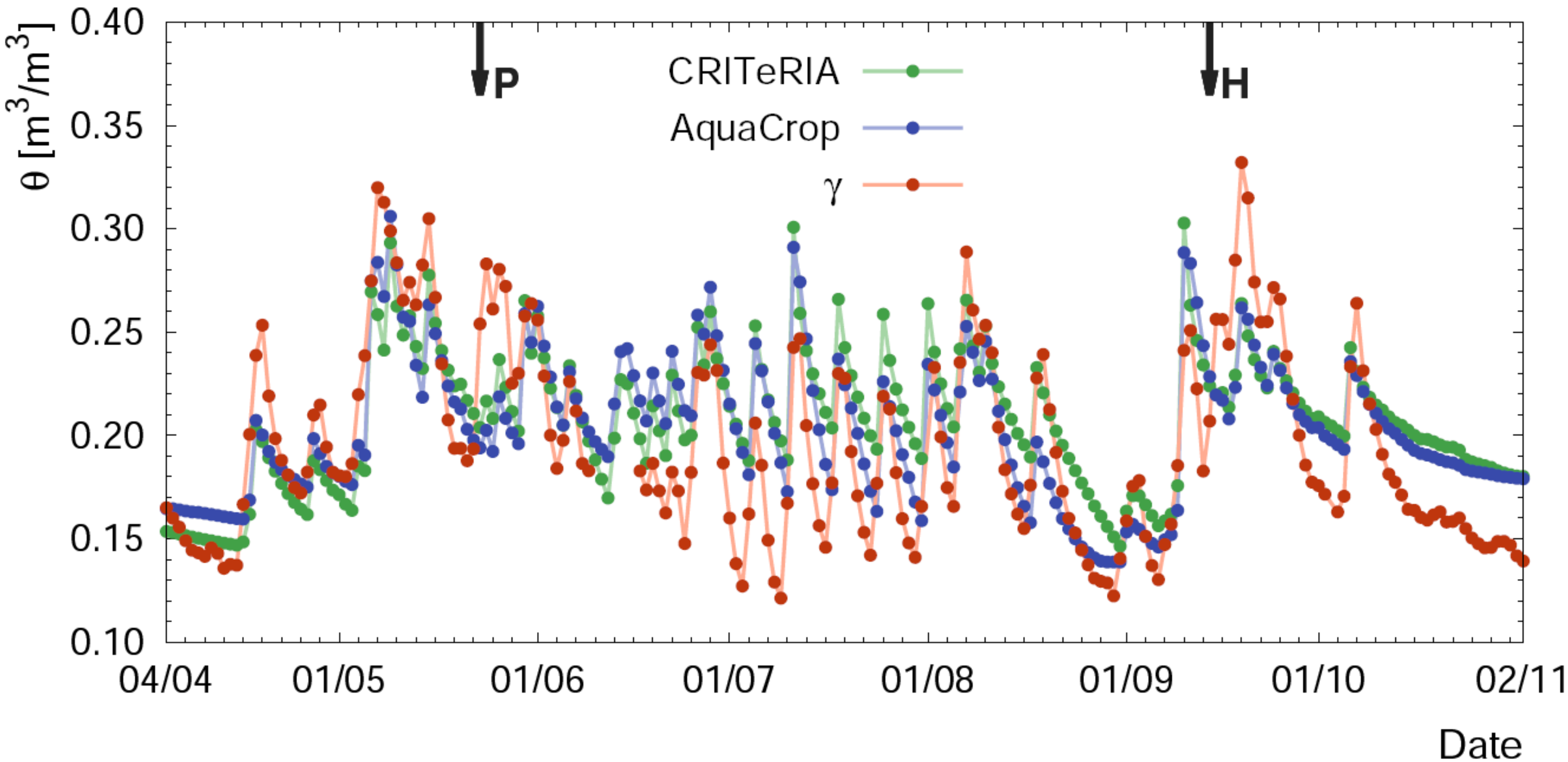

The temporal profile of water content directly measured with gamma ray follows the trends of models output: it has a great potential for tuning soil-crop numerical simulations

Main goals reached in my PhD

Implications of the accuracy of flight altitude on AGRS measurements

The uncertainty on the ground total activity due to the uncertainty on flight altitude is of about 2% when flying at 100 m

Cosmic and aircraft background radiation in AGRS surveys

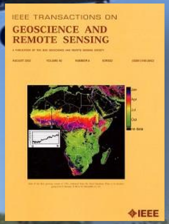

Large altitude extents AGRS surveys allow for assessing Minimum Detectable Abundances: $0.05 \cdot 10^{-2}$ g/g (K), 0.4 μg/g (U), 0.8 μg/g (Th)

AGRS for investigating atmospheric radon vertical profile

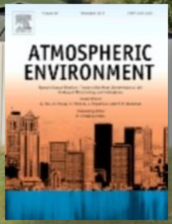

A new theoretical model of radiometric data vertical profile lead to estimate an abundance $a_{Rn} = (0.96 \pm 0.07)$ Bq/m^3 uniformly distributed up to (1318 ± 22) m

Soil water content at an agricultural site with proximal gamma ray spectroscopy

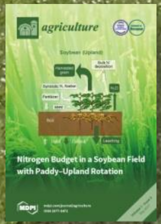

Soil water contents from gamma and gravimetric measurements are in excellent agreement, compatible at 1σ level

Perspectives

- Estimate the implications of the uncertainty due to the morphological corrections on the uncertainty budget of ground abundances determined with AGRS surveys
- Investigate the potentialities of the integration of AGRS measurements with data acquired in different energy ranges of the electromagnetic spectrum

- Estimate systematic uncertainties in in-situ gamma-ray measurements introduced by atmospheric radon
- Development and validation of a theoretical model for radon exhalation from the soil in different day-time periods

- Investigate diurnal cycles of proximal gamma-ray spectroscopy measurements in relation to environmental and weather data
- Study of the possible correlations of radiometric data with soil physical and chemical parameters


Thank you
CAMPOBASSO

List of publications

Albéri, M., Baldoncini, M., Bottardi, C., Chiarelli, E., Fiorentini, G., Raptis, K. G. C., Realini, E., Reguzzoni, M., Rossi, L., Sampietro, D., Strati, V. and Mantovani, F. Accuracy of flight altitude measured with low-cost GNSS, radar and barometer sensors: implications on airborne radiometric surveys. **Sensors** (Basel) (2017) 17(8), 1889. DOI: 10.3390/s17081889. (IF: 2.964)

Baldoncini, M., **Albéri, M.**, Bottardi, C., Raptis, K. G. C., Minty, B., Strati, V. and Mantovani, F. Exploring atmospheric radon with airborne gamma-ray spectroscopy. **Atmospheric Environment** (2017). DOI: 10.1016/j.atmosenv.2017.09.048 (IF: 3.948)

Baldoncini, M., **Albéri, M.**, Bottardi, C., Raptis, K. G. C., Minty, B., Strati, V. and Mantovani, F. Airborne gamma-ray spectroscopy for modeling cosmic radiation and effective dose in the lower atmosphere. **IEEE Transactions on Geoscience and Remote Sensing** (2017) DOI: 10.1109/TGRS.2017.2755466. (IF: 4.942)

Kaçeli Xhixha, M., **Albéri, M.**, Baldoncini, M., Bezzon, G.P., Buso, G.P., Callegari, I., Casini, L., Cuccuru, S., Fiorentini, G., Guastaldi, E., Mantovani, F., Mou, L., Oggiano, G., Puccini, A., Rossi Alvarez, C., Strati, V., Xhixha, G., Zanon, A.. Map of the uranium distribution in the Variscan Basement of Northeastern Sardinia. **Journal of Maps** (2015). DOI:10.1080/17445647.2015.1115784 (IF: 1.435)

Xhixha, G., **Albéri, M.**, Baldoncini, M., Bode, K., Bylyku, E., Cfarku, F., Callegari, I., Hasani, F., Landsberger, S., Mantovani, F., Rodriguez, E., Shala, F., Strati, V., Kaçeli Xhixha, M. Calibration of HPGe detectors using certified reference materials of natural origin. **Journal of Radioanalytical and Nuclear Chemistry** (2015). DOI: 10.1007/s10967-015-4360-6 (IF:3.698)

D. Mesa, R. Gratton, A. Zurlo, A. Vigan, R. U. Claudi, **M. Albéri**, J. Antichi, A. Baruffolo, J.-L. Beuzit, A. Boccaletti, M. Bonnefoy, A. Costille, S. Desidera, K. Dohlen, D. Fantinel, M. Feldt, T. Fusco, E. Giro, T. Henning, M. Kasper, M. Langlois, A.-L. Maire, P. Martinez, O. Moeller-Nilsson, D. Mouillet, C. Moutou, A. Pavlov, P. Puget, B. Salasnich, J.-F. Sauvage, E. Sissa, M. Turatto, S. Udry, F. Vakili, R. Waters and F. Wildi, Performance of the VLT Planet Finder SPHERE - II. Data analysis and results for IFS in laboratory. **Astronomy & Astrophysics**, 576 (2015) A121 DOI:/10.1051/0004-6361/201423910 (IF: 5.014)